Effect of the water-soluble matrix of nanometer pearl powder on the osteogenic differentiation of hFOB1.19 cells

XINGHUANYU XU[1,2], LIN LIU[1], WENBAI ZHANG[1] and PU XU[1]

[1]Department of Oral Implantology, Stomatology Center, Affiliated Haikou Hospital, Xiangya Medical College, Central South University, Haikou, Hainan 570100, P.R. China; [2]Department of Oral and Maxillofacial Surgery, Xiangya Stomatological Hospital, Xiangya School of Stomatology, Central South University, Changsha, Hunan 410000, P.R. China

Received July 10, 2024; Accepted March 21, 2025

DOI: 10.3892/etm.2025.13003

Abstract. Pearl powder, especially its main effective component water-soluble matrix (WSM), can promote bone formation. The present study analyzed the effect of various WSM concentrations on the osteogenic differentiation of hFOB1.19 cells. The WSM of nanometer pearl powder (NPP) was obtained through the water extraction method. hFOB1.19 cells were then cultured with WSM at concentrations of 0, 10, 20 and 40 μg/ml. Thereafter, alkaline phosphatase (ALP) activity and alizarin red staining were analyzed to detect the effects of WSM on the osteogenic differentiation and mineralization of hFOB1.19 cells. In addition, type I collagen, osteocalcin, osteopontin and Runt-associated transcription factor 2 mRNA and protein expression levels during osteogenic differentiation were measured through reverse transcription-quantitative PCR and western blotting. Following WSM treatment, ALP activity, alizarin red staining of mineralized nodules and osteoblast-related protein expression levels were all found to be elevated in hFOB1.19 cells. In conclusion, these results suggested that NPP WSM could promote the differentiation and mineralization of hFOB1.19 cells within the tested concentration range to induce an osteogenic effect.

Introduction

Pearl powder is a Traditional Chinese Medicine with a variety of active substrates, which can be applied for numerous processes, such as wound healing and bone repair, rendering it a promising biological agent. The nacre organic matrix, an active component of pearl powder, mainly regulates the mineralization of bivalve mollusks (1). The nacre is an organic/inorganic complex that is not too dissimilar to human bone tissues (2). In addition, the organic matrix of pearl powder is the processed product of pearl powder (3). The solvent capable of dissolving the organic components of the medium is typically combined with the pearl powder components, which are obtained by centrifugation, freezing and other methods such as supercritical CO_2 extraction and enzyme-acid extraction. The insoluble matrix components are then removed and the soluble organic matrix is retained (4). Pearl powder has been applied in traditional Chinese medicine and cosmetics for >1,000 years (5). Chiu *et al* (6) previously found that pearl powder extract can prolong the life of *Caenorhabditis elegans*. Additionally, in the same study, 20 subjects (aged 38-50 years) were administered pearl powder capsules and placebo. After 10 weeks of treatment, antioxidant-related indices were found to be increased in plasma samples, suggesting that pearl powder has antioxidant activity (6). This also suggests the potential of pearl powder for the treatment of age-related degenerative diseases. Chen *et al* (7) conducted *in vitro* and *in vivo* experiments with pearl powder with different particle sizes, and found that the mixed preparation of pearl powder/glycerol/normal saline could promote the proliferation and migration of fibroblasts, accelerate wound closure and promote skin angiogenesis in full-thickness skin excision wounds in Sprague-Dawley rats and shaped dermal wounds in New Zealand rabbits. In another study, Zhang *et al* (8) assessed the effects of pearl powder and its extract on the motor ability and anticonvulsant ability of mice, where the results showed that rearing was inhibited in ordinary mice, whilst the convulsant latency of pentylenetetrazol model mice was prolonged. These results provide the basis for the development of sedative drugs based on pearl powder.

The bone tissue is comprised of a diverse range of cell components, namely preosteoblasts, osteoblasts and osteoclasts, which jointly modulate the growth and absorption of bone tissues (9). Osteoblasts, derived from bone marrow mesenchymal stem cells (MSCs), serve a function in osteogenesis and serve a critical role during bone remodeling. Specifically, osteoblasts promote bone tissue formation by secreting organic matrix and regulating calcification (10). Certain cytokines, such as TNF-α, have an important role in regulating bone metabolism (11). This cytokine, produced mainly by activated macrophages, T lymphocytes, activated

Correspondence to: Dr Pu Xu, Department of Oral Implantology, Stomatology Center, Affiliated Haikou Hospital, Xiangya Medical College, Central South University, 43 Renmin Avenue, Meilan, Haikou, Hainan 570100, P.R. China
E-mail: hnxupu@163.com

Key words: nanometer pearl powder, water-soluble matrix, hFOB1.19 cells, osteoblast, osteogenic differentiation

macrophages, monocytes, $CD4^+$ T cells, B cells, neutrophils and mast cells, induces apoptosis of leukemia cell lines *in vitro* and stimulates osteoclast activation, and TNFα promotes osteoblast differentiation and bone formation by polarizing macrophages to secrete insulin like 6 and Jagged1, while anti-TNF treatment may indirectly affect osteoblast activity by inhibiting the expression of these factors, which in turn promotes bone degradation (12,13). Other factors, such as transcriptional coactivator Yes1-associated transcriptional regulator (YAP), also serve important roles in osteogenesis. YAP acts as a key molecular bridge connecting the mechanical microenvironment (substrate size/spatial features) to osteogenic differentiation, directly mediating the sequential regulation of MSC and osteoblast differentiation through focal adhesion-dependent cytoskeletal tension (regulated by F-actin and phospho-myosin light chain 2) that drives its nuclear localization. This mechanoregulatory role has further been confirmed in cytoskeleton disruption assays (14).

As an active component of nacre pearls, nacre powder organic matrix has been documented to regulate the mineralization of bivalve mollusks such as *Pinctada* spp. and *Crassostrea gigas*, where its effects on osteoblasts has been extensively studied (1,15).

Pearl powder is similar to nacre powder. Pearl powder and nacre powder differ in their origins: Natural pearls form when foreign irritants (such as sand or parasites) accidentally enter oysters and become progressively mineralized under nacreous encapsulation (16). By contrast, the nacreous layer constitutes a laminated composite material secreted by mantle epithelial cells, characterized by alternating deposition of calcium carbonate crystals and chitinous proteins (17). Both materials share similar chemical compositions, containing 95% calcium carbonate and 5% organic components, including diverse amino acids, trace elements, vitamins and bioactive peptides (18,19). Notably, their core bioactive constituents derive from the organic matrix, which is a complex system comprising proteins, polypeptides, glycoproteins, chitin, lipids and pigments (18,19). A proteomic study has revealed compositional differences between nacre from *Pinctada maxima* (Kamingi shell) and that of cultured pearls in protein profiles (20). This structure confers osteoinductive properties, enabling stimulation of osteoblast differentiation via the bone morphogenetic protein 2/Smad signaling pathway and biomimetic mineralization, making it suitable for bone regeneration applications (21). However, to the best of our knowledge, research on the effect of the organic matrix extracted from pearl powder on osteoblasts remains scarce. In the present study, hFOB1.19 cells were cultured with the water-soluble matrix (WSM) derived from nanometer pearl powder (NPP) to analyze its possible effects on the osteogenic differentiation of these osteoblasts. It is hoped that the present study will encourage the application of pearl powder for promoting bone formation in the clinic. In particular, pearl powder WSM can be applied in artificial bone materials or for the treatment of osteoporosis.

Materials and methods

NPP WSM preparation. Micron-grade pearl powder (Hainan Jingrun Pearl Co., Ltd.) was first ground into nano-grade pearl powder. Briefly, a CNB-T1L nanorstick needle mill (Dongguan Kangbo Machinery Co. Ltd.) was used, sterile distilled water was used for cleaning to eliminate potential contaminants, anhydrous ethanol was used as the medium, the rotation speed of the main engine was set at 540 x g, the feed pressure was 0.35 kPa, the mass/volume ratio was 1:15 (g/ml) to add pearl powder, and mechanical grinding was performed for 1 h at room temperature (25˚C). A uniform nanosuspension was obtained. The slurry was oven-dried at 60˚C for 24 h, manually pulverized using a ceramic mortar in a clean workbench, sieved through a 120 mesh, and stored as uniform nanopearl powder in sterile containers. After freeze drying and irradiation sterilization, the pearl powder was mixed with Milli-Q ultra-pure water (MilliporeSigma) at a ratio of 1:2 (g/ml), before the supernatant was collected by centrifugation (500 x g; 20 h) at room temperature (25˚C). The sample was later filtered with a 0.22-μm strainer and freeze-dried to obtain the WSM powder, which was then dissolved in PBS. The stock WSM protein concentration was determined using the BCA protein quantitative kit and the stock solution was stored at 4˚C. The protein concentration of WSM calculated by the BCA protein assay method was 2.689 mg/ml. It was calculated that 134.47 mg protein could be extracted per 100 g of nano-pearl powder. WSM was then diluted to 10, 20 and 40 μg/ml before the subsequent experiments.

hFOB1.19 cell culture. hFOB1.19 cells (cat. no. CL-0353; Procell Life Science & Technology Co., Ltd.) were cultivated in DMEM/F12 (cat. no. C11330500BT; Gibco; Thermo Fisher Scientific, Inc.) containing 10% FBS (cat. no. 10099141C; Gibco; Thermo Fisher Scientific, Inc.) and 0.3 mg/ml G418 [cat. no. 1811031; Geneticin™ Selective Antibiotic (G418 Sulfate); Gibco; Thermo Fisher Scientific, Inc.] in a 5% CO_2 atmosphere at 34˚C. The medium was changed every 2 days. After reaching 80-90% confluency, trypsin (Gibco; Thermo Fisher Scientific, Inc.) was added to digest the cells and 1:2 passaging was performed. In the experimental groups, solutions of 10, 20 and 40 μg/ml WSM were added to the cells, whilst an equal amount of complete medium was added to the control group. Co-cultures were incubated for 1, 4, 7 and 14 days as required. The cultures were incubated at 34˚C in a 5% CO_2 atmosphere.

Cell differentiation detection based on alkaline phosphatase (ALP) activity. Cells in passage 3 were selected and inoculated into a 24-well plate at $2x10^5$ cells/well. The cells were grouped as aforementioned and three replicate wells were set up for every group. The culture medium was discarded when the cells attached to the well, before WSM was added. After intervention for 1, 4 and 7 days at 34˚C with 5% CO_2, the medium was discarded, and subsequent procedures were conducted according to the ALP kit manufacturer's protocol (cat. no. A059-1-1; Nanjing Jiancheng Bioengineering Institute). The absorbance was measured using an absorbance reader (800TS; BioTek; Agilent Technologies, Inc.).

Cell mineralization detection by alizarin red staining. Cells in passage 3 were selected and inoculated into 6-well plates at $5x10^6$ cells/well. Cell grouping and culture were performed following the same method as those performed for measuring

ALP activity. Medium was removed after culturing for 7 and 14 days, before the cells were washed three times with PBS for 5 min each and fixed with 4% paraformaldehyde for 30 min at 25˚C. After washing with PBS three times again, 4 ml 2% alizarin red solution (cat. no. DF0563; Yingxin Biotechnology, Co., Ltd.) was added to every well for 15 min at ambient temperature (25˚C) for staining. Following further washing with PBS three times, the calcified nodules formed were monitored using an LED light microscope (Nikon TS100; Nikon Corporation), before images were collected and the relative absorbance value (595 nm) of the mineralized area (ImageJ Software 1.54a; National Institutes of Health) was determined for statistical analysis.

Relevant osteogenic gene expression levels measured by reverse transcription-quantitative PCR (RT-qPCR). Cells in passage 3 were selected and inoculated into a 6-well plate at $5x10^6$ cells/well. Cell grouping and culture were conducted with the same method as those performed for measuring ALP activity. The medium was removed following a 7-day culture and TRNzol Universal Reagent (cat. no. DP424; Tiangen Biotech Co., Ltd.) was utilized to extract the total cellular RNA. The RNA concentration and purity were determined by an ultraviolet spectrophotometer (BioTek; Agilent Technologies, Inc.). Subsequently, 0.85 μg RNA was reverse transcribed using a PrimeScript™ RT Master Mix (Perfect Real Time; cat. no. RR036A; Takara Bio, Inc.) to synthesize cDNA at 37˚C for 15 min and 85˚C for 5 sec. The cDNA was used as the template and amplified according to the instructions of the Hieff® qPCR SYBR Green Master Mix (cat. no. 11201ES08; Shanghai Yeasen Biotechnology Co., Ltd.). The relative mRNA expression levels of type I collagen (Col-I), osteocalcin (OCN), osteopontin (OPN) and Runt-associated transcription factor 2 (Runx-2) were detected by $2^{-\Delta\Delta Cq}$ method, with GAPDH as the reference gene (22). Table I displays the primers. The qPCR conditions included pre-denaturation at 95˚C for 5 min, followed by 40 cycles of denaturation at 95˚C for 10 sec and annealing at 60˚C for 30 sec.

Relevant osteogenic protein expression levels detected by western blotting. Western blotting was performed according to Jurisic *et al* (23). Cells in passage 3 were selected and inoculated into a 6-well plate at $5x10^6$ cells/well. Cell grouping and culture were conducted with the same method as those performed for measuring ALP activity. The medium was removed following a 7-day culture, before cellular proteins were extracted from every group using RIPA lysis buffer (cat. no. BL504A; Biosharp Life Sciences). The protein concentration was quantified using the BCA method. Equal amounts of protein (50 μg per lane) were resolved by 12% SDS-PAGE and electrophoretically transferred onto 0.22-μm PVDF membranes. The proteins were transferred onto PVDF membranes, which were subsequently blocked with 5% skimmed milk in TBS with 20% Tween 20 (cat. no. ST1726; Beyotime Institute of Biotechnology) for 1 h at room temperature (25˚C). The membranes were then incubated with the primary antibodies at 4˚C overnight. The primary antibodies (all from Affinity Biosciences) were as follows: Rabbit polyclonal Col-I (cat. no. AF7001; 1:1,000), rabbit polyclonal OCN (cat. no. DF12303; 1:1,000), rabbit polyclonal OPN (cat. no. AF0227; 1:1,000); rabbit polyclonal Runx-2 (cat. no. AF5186; 1:1,000) and rabbit polyclonal GAPDH (cat. no. AF7021; 1:10,000). The membrane was then incubated with goat anti-rabbit IgG (H + L) HRP secondary antibody (cat. no. S0001; 1:10,000; Affinity Biosciences, Ltd.) at room temperature for 1 h. The Affinity™ ECL kit (femtogram) (cat. no. KF8003; Affinity Biosciences, Ltd.) was used for band exposure development. Finally, ImageJ software (version1.53e; National Institutes of Health) was used for the semi-quantitative analysis of the protein bands, before the ratio between the target protein and the internal reference protein (GAPDH) was calculated for statistical analysis.

Statistical analysis. Each assay was conducted three times. The experimental data are presented as the mean ± standard deviation. Statistical analysis and mapping were performed using GraphPad Prism 8.2.1 software (Dotmatics). Data among several groups were compared by one-way analysis of variance. The Tukey post hoc test was used for analysis of variance. $P<0.05$ was considered to indicate a statistically significant difference.

Results

Effects of different NPP WSM concentrations on the early osteogenic differentiation of cells. The ALP activity was not found to be significantly different among all experimental groups after 1 day of treatment with WSM (Fig. 1). Following WSM treatment for 4 and 7 days, the ALP activity was enhanced as the WSM concentration increased, as significant differences were detected between the groups with different WSM concentrations and the control group. On day 4, significant differences were observed between all treatment groups and the control group, demonstrating a concentration-dependent increase in ALP activity. By day 4, there were statistically significant differences between each treatment group and the control group, and between all treatment groups. By day 7, statistically significant variations were noted not only between each treatment group and the control group, but also between the 10 μg/ml group and both the 20 and 40 μg/ml groups. However, no significant difference was detected between the 20 and 40 μg/ml groups on day 7 (Fig. 1). Therefore, these data suggest that WSM promoted the secretion and activity of ALP in hFOB1.19 cells.

Effects of different NPP WSM concentrations on cell mineralization. After 7 days of culture, mineralization in the 20 and 40 μg/ml WSM groups was found to be significantly increased compared with that in the blank control group. Following a 14-day culture, compared with that in the blank control group, the area of mineralized nodules in the 10-40 μg/ml WSM groups was significantly elevated, particularly in the 40 μg/ml WSM group. However, there was no difference among the WSM treatment groups on day 14 (Figs. 2 and 3).

Effects of different NPP WSM concentrations on osteogenic gene expression. As shown in Fig. 4, after 7 days of culture, the expression of target genes (Col-I, OCN, OPN and Runx-2) in the 10-40 μg/ml WSM groups was found to be significantly increased compared with that in the blank control group. Additionally, the target gene mRNA levels in the 40 μg/ml

Table I. Primers designed for reverse transcription-quantitative PCR.

Gene	Sequence (5'-3')
GAPDH	CACCCACTCCTCCACCTTTGAC
	GTCCACCACCCTGTTGCTGTAG
Collagen-I	CCTGCCTGGTGAGAGAGGT
	AGTAGCACCATCATTTCCACGA
Osteocalcin	AGCAAAGGTGCAGCCTTTG
	GCGCCTGGGTCTCTTCACT
Osteopontin	GACCTGAACGCGCCTTCTGAT
	ATCTGGACTGCTTGTGGCTGTG
Runt-associated transcription factor 2	CCGCTTCTCCAACCCACGAAT
	TGGCAGGTAGGTGTGGTAGTGA

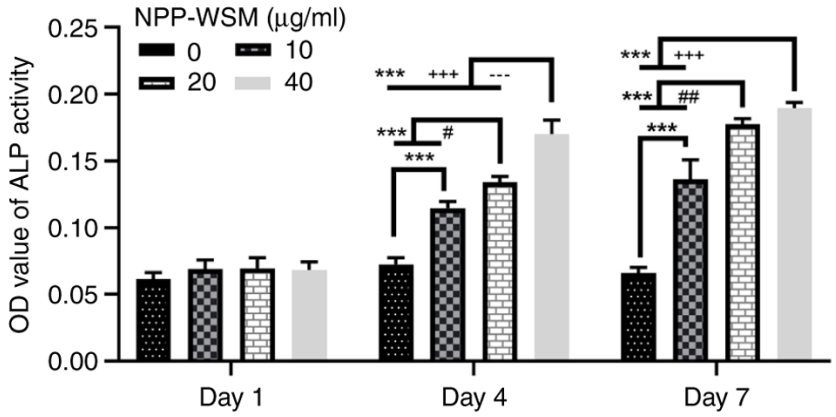

Figure 1. Effects of different concentrations of WSM on the ALP activity of hFOB1.19 cells. A high concentration of WSM (40 μg/ml) significantly enhanced the ALP activity of hFOB1.19 cells. WSM stimulates hFOB1.19 cell differentiation. ALP activity, a marker of osteogenic differentiation, was measured in cells treated with WSM (0, 10, 20 and 40 μg/ml) for 1, 4 and 7 days. Data are presented as the means ± standard deviation, n=4. ***P<0.001 (0 μg/ml vs. all other groups); $^{\#}$P<0.05 and $^{\#\#}$P<0.01 (10 vs. 20 μg/ml); $^{+++}$P<0.001 (10 vs. 40 μg/ml); $^{---}$P<0.001 (20 vs. 40 μg/ml). WSM, water-soluble matrix; ALP, alkaline phosphatase; OD, optical density.

WSM group were significantly elevated compared with those in the 10 and 20 μg/ml WSM groups.

Effects of different NPP WSM concentrations on osteogenic protein expression. As shown in Figs. 5 and 6, target protein (Col-I, OCN, OPN and Runx-2) expression in the 10, 20 and 40 μg/ml WSM groups was found to be increased following 7 days of culture compared with that in blank control group. However, the protein expression level in the 40 μg/ml group was not significantly different compared with that in the 20 μg/ml group.

Discussion

Remodeling of the bone tissue is regulated by a variety of cytokines, where the key to maintaining the integrity of bone tissue is to regulate the homeostasis between osteoblasts and osteoclasts (24). Pro-osteoclast cytokines include TNF-α and the IL family, whereas anti-osteoclast cytokines mainly include IFN-α, IFN-β and IFN-γ (25). These aforementioned factors serve a key role in osteoclast formation through the interaction between the bone and the immune system (26). Lan *et al* (27) previously studied the regulatory effect of hydrolyzed seawater pearl tablet (HSPT) on Th1/Th2 imbalance in immunosuppressed mice induced by cyclosporin A. The results showed that the protein and mRNA expression levels of Th1 cytokines IL-2 and IFN-γ were increased in mice treated with HSPT. HSPT may ameliorate Th1/Th2 imbalance under immunosuppressive conditions by upregulating the expression of Th1 cytokines, IL-2 and IFN-γ. Future studies should further explore whether these immunomodulatory effects indirectly influence bone metabolism or the balance between osteoblast and osteoclast activity.

As a natural polymer, pearl powder is currently a topic of intense research in the field of bone tissue engineering (28-30). The composition of pearl powder is similar to that of nacre powder (31). Previous studies have shown that pearl powder and artificial bone materials containing pearl powder have osteogenic effects both in *in vivo* and *in vitro* (32,33). However, the majority of recent studies have focused on the osteogenic application of nacre powder matrix (15,34), whilst to the best of our knowledge, studies on the effect of pearl powder matrix on osteoblasts remained scarce. The nacre organic matrix is a key substance in regulating the mineralization of bivalve

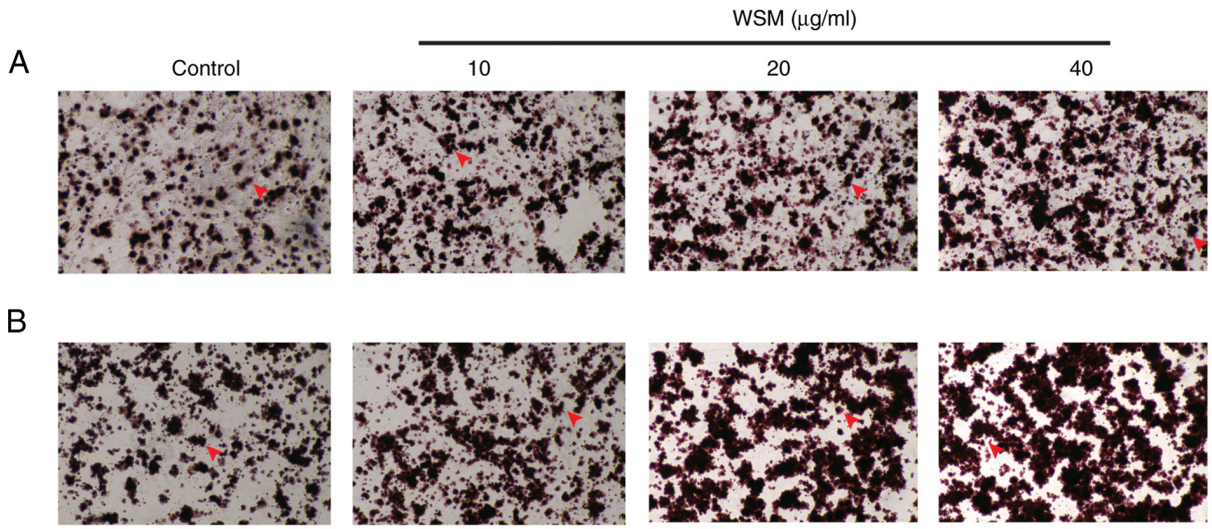

Figure 2. Alizarin red staining images of mineralized nodules. WSM increased alizarin red staining in a concentration-dependent manner, according to the area of mineralized nodules (magnification, x200). High concentrations of WSM could increase the degree of hFOB1.19 cell mineralization. The red arrow marks the calcified nodules. (A) 7 and (B) 14 days. WSM, water-soluble matrix.

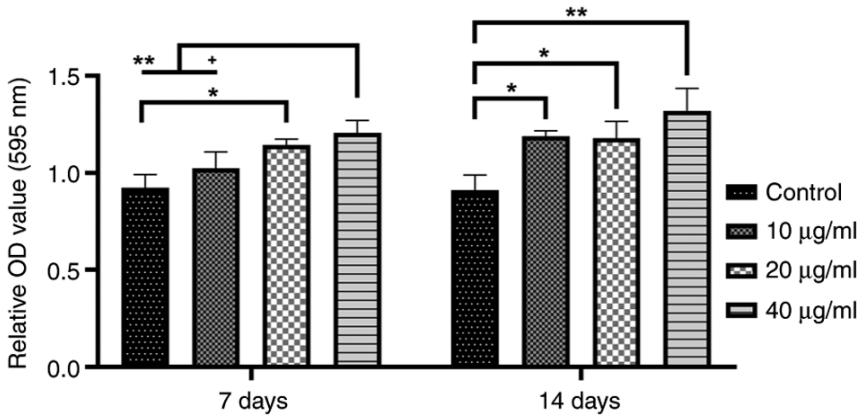

Figure 3. Alizarin red staining assay was semi-quantified to measure cell mineralization following water-soluble matrix treatment (0, 10, 20 and 40 μg/ml) for 7 and 14 days. Data are presented as the means ± standard deviation, n=4. *P<0.05 and **P<0.01 (0 μg/ml vs. all other groups); $^{+}$P<0.05 (10 vs. 40 μg/ml). OD, optical density.

mollusks (1). The invertebrate mineralization process and mammalian bone calcification have similar signaling pathways where the signaling molecules have similar protein domains. Previous studies have shown that the NPP organic matrix can promote the differentiation of osteoblasts (35,36). Pearl powder has also been shown to promote collagen production and serve a role in wound healing following skin injuries (7,37). In particular, pearl powder and composite materials constructed with pearl powder have been documented to promote osteogenesis in a variety of cell lines, such as mouse bone marrow MSCs (38) and rat bone MSCs (39).

Nanomaterials have properties that materials of general size (>1 μm) do not have. Nano-treatment of pearl powder or pearl layer powder not only retains the effective components of pearl powder, but also results in an improved osteogenic effects (40). A previous review examined the effects of four inorganic or metallic nanoparticles widely used as biomaterials, namely hydroxyapatite, silica, silver and calcium carbonate, on the osteogenic and lipogenic differentiation of MSCs (41). The size of the materials can affect cell function, revealing that these materials have rich application prospects on the nanoscale (41). There have been a number of studies on the use of NPP and its scaffold materials. Chen *et al* (7) previously found that NPP can promote the proliferation and migration of skin cells, accelerate wound healing and improve the biomechanical strength of healed skin in both *in vivo* and *in vitro* experiments. In addition, Yang *et al* (42) constructed a NPP/poly (lactide-co-glycolide) biocomposite scaffold, which promoted the uniform seeding, adhesion and proliferation of MC3T3-E1 cells, which is a pre-osteoblastic cell line derived from mouse calvaria, possessing osteogenic differentiation potential. Therefore, NPP is relatively reproducible and provides structural features that can enhance the formation of bone tissues. A previous study also demonstrated that scaffolds constructed with NPP had osteogenic effects (30).

The pearl powder matrix can be obtained according to the different media, where the finished products are

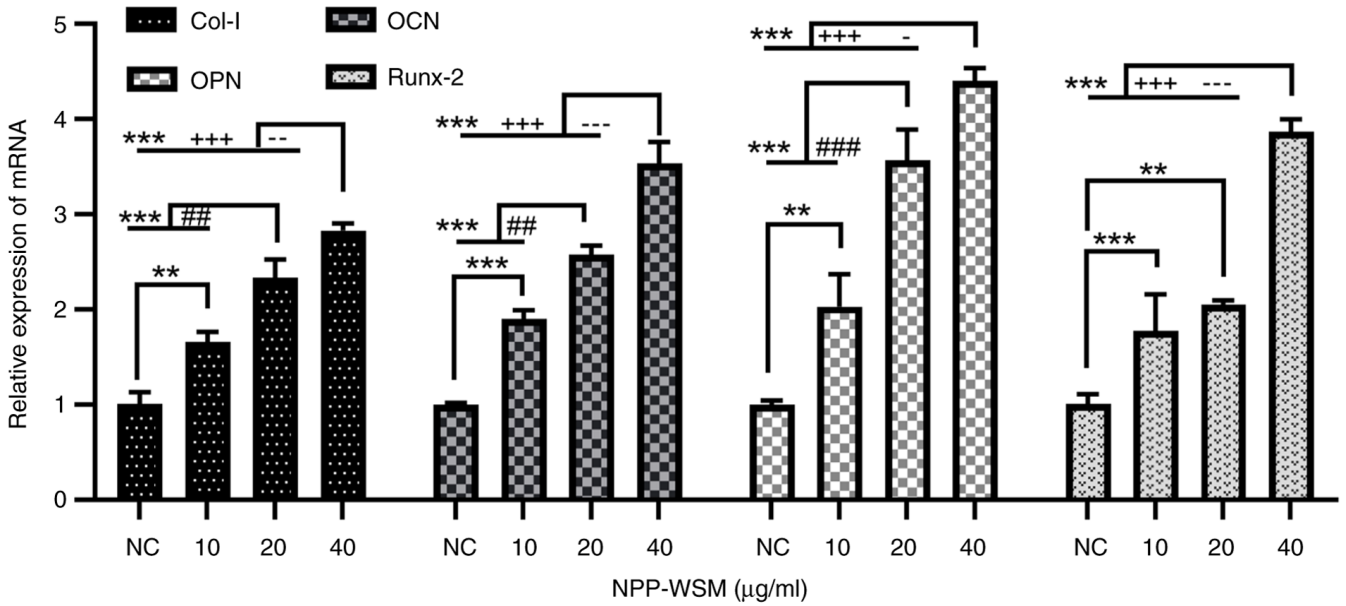

Figure 4. mRNA expression of osteogenic genes in each WSM treatment group (0, 10, 20 and 40 μg/ml) measured through reverse transcription-quantitative PCR. Data are presented as the means ± standard deviation, n=4; **P<0.01 and ***P<0.001 (0 μg/ml vs. all other groups); $^{\#\#}$P<0.01 and $^{\#\#\#}$P<0.001 (10 vs. 20 μg/ml); $^{-}$P<0.05, $^{--}$P<0.01 and $^{---}$P<0.001 (20 vs. 40 μg/ml); $^{+++}$P<0.001 (10 vs. 40 μg/ml). WSM, water-soluble matrix; Col-I, type I collagen; OCN, osteocalcin; OPN, osteopontin; Runx-2, Runt-associated transcription factor 2; NC, negative control.

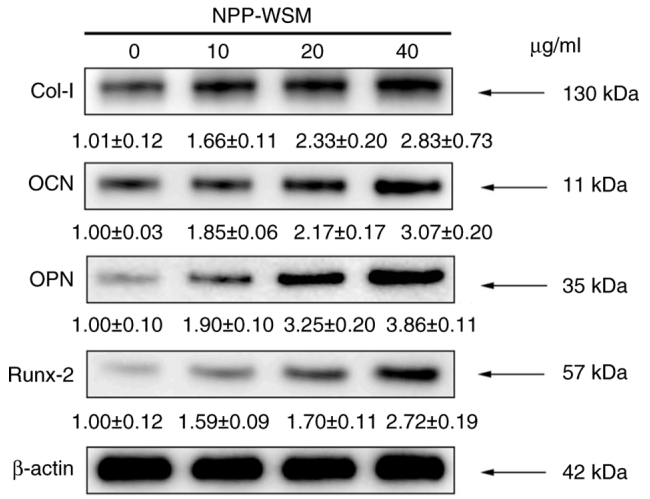

Figure 5. Representative western blotting images. Compared with the those in the control group, there were significant differences in the expression of bone-related proteins after water-soluble matrix treatment, where certain differences were also found among groups of 10, 20 and 40 μg/ml. Col-I, type I collagen; OCN, osteocalcin; OPN, osteopontin; Runx-2, Runt-associated transcription factor 2.

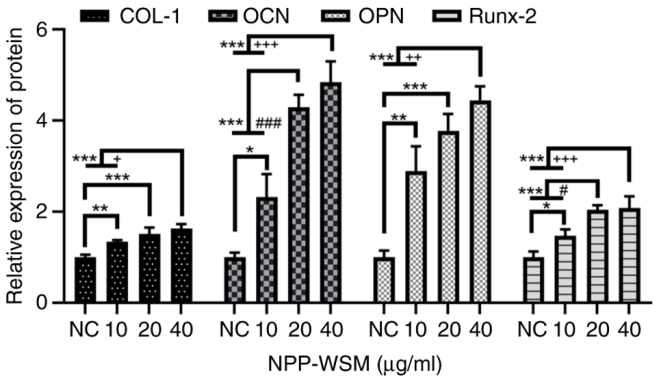

Figure 6. Osteogenic protein expression detected in each group following WSM treatment (0, 10, 20 and 40 μg/ml) by western blotting. There were significant differences in the expression of bone-related proteins following WSM treatment. Data are presented as the means ± standard deviation, n=4. *P<0.05, **P<0.01 and ***P<0.001 (0 μg/ml vs. all other groups); $^{\#}$P<0.05 and $^{\#\#\#}$P<0.001 (10 vs. 20 μg/ml); $^{+}$P<0.05, $^{++}$P<0.01 and $^{+++}$P<0.001 (10 vs. 40 μg/ml). Col-I, type I collagen; OCN, osteocalcin; OPN, osteopontin; Runx-2, Runt-associated transcription factor 2; NC, negative control; WSM, water-soluble matrix.

termed 'WSM', 'water-insoluble matrix' and 'acid-soluble protein' (31). WSM has a high water solubility and can be widely used in cell assays and skin wound healing experiments. The active ingredients of WSM are rapidly absorbed by cells and skin, making it the pearl powder-related product that is closest to clinical application (7,32,37,38,43). Liu *et al* (44) previously obtained the WSM of pearl powder using a CO_2 supercritical extraction system, where the subsequent product was found to promote the migration and proliferation of fibroblasts. In rats with skin defects, 5 and 10 mg/ml WSM had a marked effect on wound healing (the healing area of the wound was higher than that in the control group), whilst 15 mg/ml had a poor effect (the wound healing area was not as good as in other groups). It was speculated that a high WSM concentration may have toxic effects on the skin, since the Masson's staining of tissues has also shown abundant collagen hyperplasia (38). In another study, Dai *et al* (45) extracted the WSM from pearl powder and further fractionated it into MR14 (>14 kDa), MR3-14 (3-14 kDa) and MR3 (<3 kDa) based on molecular weight. The authors found that WSM and MR14 promoted proliferation, while all fractions enhanced collagen deposition in primary oral fibroblasts from BALB/c mice.

In a previous study, NPP WSM was found to enhance autophagy in MC3T3-E1 cell lines to promote their differentiation through the MEK/ERK signaling pathway (46). In the present study, NPP WSM was applied to human cells. Specifically, NPP WSM was further applied to hFOB1.19 cells, where the results demonstrated that there was no significant difference in ALP activity among all experimental groups after 1 day of incubation, which may be due to the insufficient time allowed for osteoblast differentiation. On days 3 and 7, the ALP activity of the treated hFOB1.19 cells was significantly enhanced, where the effect of WSM on the osteogenic differentiation of hFOB1.19 cells on day 7 was stronger compared with that on day 3. These results suggest that 10, 20 and 40 μg/ml NPP WSM can promote the osteogenesis of hFOB1.19 cells. Col-I, OCN, OPN and Runx-2 are biomarkers commonly used in biological experiments and clinical examinations to reflect the effects of bone formation (43). In the present study, the expression levels of Col-I, OCN, OPN and Runx-2 were found to be significantly increased in hFOB1.19 cells treated with NPP WSM, suggesting that NPP WSM may achieve osteogenic effects by regulating the expression of these proteins. In two other previous studies on skin wound healing, Col-I expression was observed to be increased in mice fibroblasts treated with pearl powder WSM (44,45), whereas in another previous study Col-I and Runx-2 expression levels were also reported to be increased in MC3T3-E1 cells treated with NPP WSM (46). These results are consistent with those in the present study.

However, there are a number of limitations in the present study. The signaling pathways associated with NPP WSM osteogenesis were not investigated further. In addition, a positive control group with a known substance that can definitively induce osteogenesis was not included.

In conclusion, the results of the present study suggest that NPP WSM may promote the osteogenic differentiation of hFOB1.19 cells, by regulating the expression of the osteogenic factors, Col-I, OCN, OPN and Runx-2, in a dose-dependent manner. These results suggest that NPP WSM could be further explored in future studies for its potential application in oral implants addressing insufficient alveolar ridge bone mass. In follow-up studies, a bone defect model in animals is required, with implantation surgeries, to explore the effective concentration and therapeutic effect of NPP WSM *in vivo*, with aims of eventual clinical studies.

Acknowledgements

Not applicable.

Funding

The present study was funded by the China National Natural Science Foundation Project (grant no. 82060194), Hainan Province Key Research and Development Project (grant no. ZDYF2022SHFZ119).

Availability of data and materials

The data generated in the present study may be requested from the corresponding author.

Authors' contributions

The experiments were conceived and designed by LL and PX. The experiments and analysis were performed by XX and LL. The data were analyzed by WZ and LL. The manuscript was written and revised by XX and PX. XX and PX confirm the authenticity of all the raw data. All authors read and approved the final manuscript.

Ethics approval and consent to participate

Not applicable.

Patient consent for publication

Not applicable.

Competing interests

The authors declare that they have no competing interests.

References

1. Cuif JP, Dauphin Y, Luquet G, Medjoubi K, Somogyi A and Perez-Huerta A: Revisiting the organic template model through the microstructural study of shell development in Pinctada margaritifera, the polynesian pearl oyster. Minerals 8: 370, 2018.
2. Farre B, Brunelle A, Laprévote O, Cuif JP, Williams CT and Dauphin Y: Shell layers of the black-lip pearl oyster Pinctada margaritifera: Matching microstructure and composition. Comp Biochem Physiol B Biochem Mol Biol 159: 131-139, 2011.
3. Ma Y, Qiao L and Feng Q: In-vitro study on calcium carbonate crystal growth mediated by organic matrix extracted from fresh water pearls. Mater Sci Eng C Mater Biol Appl 32: 1963-1970, 2012.
4. Almeida MJ, Milet C, Peduzzi J, Pereira L, Haigle J, Barthelemy M and Lopez E: Effect of water-soluble matrix fraction extracted from the nacre of *Pinctada maxima* on the alkaline phosphatase activity of cultured fibroblasts. J Exp Zool 288: 327-334, 2000.
5. Zhang J, Li S, Yao S, Si W, Cai L, Pan H, Hou J, Yang W, Da J, Jiang B, *et al*: Ultra-performance liquid chromatography of amino acids for the quality assessment of pearl powder. J Sep Sci 38: 1552-1560, 2015.
6. Chiu HF, Hsiao SC, Lu YY, Han YC, Shen YC, Venkatakrishnan K and Wang CK: Efficacy of protein rich pearl powder on antioxidant status in a randomized placebo-controlled trial. J Food Drug Anal 26: 309-317, 2018.
7. Chen X, Peng LH, Chee SS, Shan YH, Liang WQ and Gao JQ: Nanoscaled pearl powder accelerates wound repair and regeneration in vitro and in vivo. Drug Dev Ind Pharm 45: 1009-1016, 2019.
8. Zhang JX, Li SR, Yao S, Bi QR, Hou JJ, Cai LY, Han SM, Wu WY and Guo DA: Anticonvulsant and sedative-hypnotic activity screening of pearl and nacre (mother of pearl). J Ethnopharmacol 181: 229-235, 2016.
9. Ansari N and Sims NA: The cells of bone and their interactions. Handb Exp Pharmacol 262: 1-25, 2020.
10. Dai R, Liu M, Xiang X, Xi Z and Xu H: Osteoblasts and osteoclasts: An important switch of tumour cell dormancy during bone metastasis. J Exp Clin Cancer Res 41: 316, 2022.
11. Jurisic V, Terzic T, Pavlovic S, Colovic N and Colovic M: Elevated TNF-alpha and LDH without parathormone disturbance is associated with diffuse osteolytic lesions in leukemic transformation of myelofibrosis. Pathol Res Pract 204: 129-132, 2008.
12. Yao Z, Getting SJ and Locke IC: Regulation of TNF-induced osteoclast differentiation. Cells 11: 132, 2021.
13. Akdis M, Aab A, Altunbulakli C, Azkur K, Costa RA, Crameri R, Duan S, Eiwegger T, Eljaszewicz A, Ferstl R, *et al*: Interleukins (from IL-1 to IL-38), interferons, transforming growth factor β, and TNF-α: Receptors, functions, and roles in diseases. J Allergy Clin Immunol 138: 984-1010, 2016.

14. Zhao Y, Sun Q and Huo B: Focal adhesion regulates osteogenic differentiation of mesenchymal stem cells and osteoblasts. Biomater Transl 2: 312-322, 2021.
15. Nahle S, Lutet-Toti C, Namikawa Y, Piet MH, Brion A, Peyroche S, Suzuki M, Marin F and Rousseau M: Organic matrices of calcium carbonate biominerals improve osteoblastic mineralization. Mar Biotechnol (NY) 26: 539-549, 2024.
16. Jin C, Zhao JY, Liu XJ and Li JL: Expressions of shell matrix protein genes in the pearl sac and its correlation with pearl weight in the first 6 months of pearl formation in Hyriopsis cumingii. Mar Biotechnol (NY) 21: 240-249, 2019.
17. Commission CP and Commission SP: Pharmacopoeia of the people's Republic of China 2015. (No Title), 2015.
18. Huang F, Deng CM and Fu Z: GC-MS determination of micro-amounts of organic chemical compositions in nacre powder of Hyriopsis cumingii Lea. Phs Test Chem Anal 46: 300-302, 2010.
19. He JF, Deng Q, Pu YH, Liao B and Zeng M: Amino acids composition analysis of pearl powder and pearl layer powder. Food Ind 37: 270-273, 2016.
20. Berland S, Ma Y, Marie A, Andrieu JP, Bedouet L and Feng Q: Proteomic and profile analysis of the proteins laced with aragonite and vaterite in the freshwater mussel Hyriopsis cumingii shell biominerals. Protein Pept Lett 20: 1170-1180, 2013.
21. Green DW, Kwon HJ and Jung HS: Osteogenic potency of nacre on human mesenchymal stem cells. Mol Cells 38: 267-272, 2015.
22. Livak KJ and Schmittgen TD: Analysis of relative gene expression data using real-time quantitative PCR and the 2(-Delta Delta C(T)) method. Methods 25: 402-408, 2001.
23. Jurisic V, Srdic-Rajic T, Konjevic G, Bogdanovic G and Colic M: TNF-α induced apoptosis is accompanied with rapid CD30 and slower CD45 shedding from K-562 cells. J Membr Biol 239: 115-122, 2011.
24. Kim JM, Lin C, Stavre Z, Greenblatt MB and Shim JH: Osteoblast-osteoclast communication and bone homeostasis. Cells 9: 2073, 2020.
25. Li S, Liu G and Hu S: Osteoporosis: Interferon-gamma-mediated bone remodeling in osteoimmunology. Front Immunol 15: 1396122, 2024.
26. Jurisic V: Multiomic analysis of cytokines in immuno-oncology. Expert Rev Proteomics 17: 663-674, 2020.
27. Lan TJ, Luo X, Mo MY, Chen ZX, Luo F, Han SY, Liu P, Liang ZX, Zhang T, Li TY, *et al*: Hydrolyzed seawater pearl tablet modulates the immunity via attenuating Th1/Th2 imbalance in an immunosuppressed mouse model. J Tradit Chin Med 41: 397-405, 2021.
28. Loh XJ, Young DJ, Guo H, Tang L, Wu Y, Zhang G, Tang C and Ruan H: Pearl powder-an emerging material for biomedical applications: A review. Materials (Basel) 14: 2797, 2021.
29. Luo W, Chen Y, Chen C and Ren G: The proteomics of the freshwater pearl powder: Insights from biomineralization to biomedical application. J Proteomics 265: 104665, 2022.
30. Zhang W, Xu P, Cheng Y, Yang Y, Mao Q and Chen Z: Preparation of a nanopearl powder/C-HA (chitosan-hyaluronic acid)/rhBMP-2 (recombinant human bone morphogenetic protein-2) composite artificial bone material and a preliminary study of its effects on MC3T3-E1 cells. Bioengineered 13: 14368-14381, 2022.
31. Pei J, Wang Y, Zou X, Ruan H, Tang C, Liao J, Si G and Sun P: Extraction, purification, bioactivities and application of matrix proteins from pearl powder and nacre powder: A review. Front Bioeng Biotechnol 9: 649665, 2021.
32. Li X, Xu P, Cheng Y, Zhang W, Zheng B and Wang Q: Nano-pearl powder/chitosan-hyaluronic acid porous composite scaffold and preliminary study of its osteogenesis mechanism. Mater Sci Eng C Mater Biol Appl 111: 110749, 2020.
33. Zhang X, Du X, Li D, Ao R, Yu B and Yu B: Three dimensionally printed pearl powder/poly-caprolactone composite scaffolds for bone regeneration. J Biomater Sci Polym Ed 29: 1686-1700, 2018.
34. Li SG, Guo ZL, Tao SY, Han T, Zhou J, Lin WY, Guo X, Li CX, Diwas S and Hu XW: In vivo study on osteogenic efficiency of nHA/gel porous scaffold with nacre water-soluble matrix. Tissue Cell 88: 102347, 2024.
35. de Muizon CJ, Iandolo D, Nguyen DK, Al-Mourabit A and Rousseau M: Organic matrix and secondary metabolites in nacre. Mar Biotechnol (NY) 24: 831-842, 2022.
36. Evans JS: The biomineralization proteome: Protein complexity for a complex bioceramic assembly process. Proteomics 19: e1900036, 2019.
37. Han S, Huang D, Lan T, Wu Y, Wang Y, Wei J, Zhang W, Ou Y, Yan Q, Liu P, *et al*: Therapeutic effect of seawater pearl powder on UV-induced photoaging in mouse skin. Evid Based Complement Alternat Med 2021: 9516427, 2021.
38. Wu Y, Ding Z, Ren H, Ji M and Yan Y: Preparation, characterization and in vitro biological evaluation of a novel pearl powder/poly-amino acid composite as a potential substitute for bone repair and reconstruction. Polymers (Basel) 11: 831, 2019.
39. Du X, Yu B, Pei P, Ding H, Yu B and Zhu Y: 3D printing of pearl/$CaSO_4$ composite scaffolds for bone regeneration. J Mater Chem B 6: 499-509, 2018.
40. Qiu-Hua M and Pu X: Research progress of pearl/nacer in bone tissue repair. J Oral Sci Res 32: 311-333, 2016.
41. Yang X, Li Y, Liu X, He W, Huang Q and Feng Q: Nanoparticles and their effects on differentiation of mesenchymal stem cells. Biomater Transl 1: 58-68, 2020.
42. Yang YL, Chang CH, Huang CC, Kao WMW, Liu WC and Liu HW: Osteogenic activity of nanonized pearl powder/poly (lactide-co-glycolide) composite scaffolds for bone tissue engineering. Biomed Mater Eng 24: 979-985, 2014.
43. Rico-Llanos GA, Borrego-González S, Moncayo-Donoso M, Becerra J and Visser R: Collagen type I biomaterials as scaffolds for bone tissue engineering. Polymers (Basel) 13: 588, 2021.
44. Liu M, Tao J, Guo H, Tang L, Zhang G, Tang C, Zhou H, Wu Y, Ruan H and Loh XJ: Efficacy of water-soluble pearl powder components extracted by a CO_2 supercritical extraction system in promoting wound healing. Materials (Basel) 14: 4458, 2021.
45. Dai J.P, Chen J, Bei Y.F, Han B.X, Guo S.B and Jiang L.L: Effects of pearl powder extract and its fractions on fibroblast function relevant to wound repair. Pharm Biol 48: 122-127, 2010.
46. Cheng Y, Zhang W, Fan H and Xu P: Water-soluble nano-pearl powder promotes MC3T3-E1 cell differentiation by enhancing autophagy via the MEK/ERK signaling pathway. Mol Med Rep 18: 993-1000, 2018.